The reduction of hydrology-induced gravity variations at sites with insufficient hydrological instrumentation

MICHAL MIKOLAJ[1], BRUNO MEURERS[2] AND MARCEL MOJZEŠ[3]

1 GFZ German Research Centre for Geosciences, Section Hydrology, Potsdam, Germany (mikolaj@gfz-potsdam.de)

2 Department of Meteorology and Geophysics, University of Vienna, Vienna, Austria (bruno.meurers@univie.ac.at)

3 Department of Theoretical Geodesy, Slovak University of Technology, Bratislava, Slovakia (marcel.mojzes@stuba.sk)

Received: May 26, 2014; Revised: September 2, 2014; Accepted: February 6, 2015

ABSTRACT

The hydrology-induced gravity variation is a limiting factor in the study of geophysical phenomena with superconducting gravimeters. The goal of this paper is to analyse and reduce the hydrological effects on gravity at the Vienna (Austria) station that is a typical example of a site insufficiently equipped with hydro-meteorological sensors. The hydrological effects are studied in a local as well as a global scale. A new method for computing the local soil moisture effect is presented. This approach overcomes the lack of in situ soil moisture observations and utilizes gravity residuals in the calibration process of a local conceptual 1D soil moisture model. In addition, only a priori soil moisture variations, provided by a global hydrological model, in situ temperature, precipitation and snow height time series are required in this approach. The coupling of the calibration process to gravity residuals increases the sensitivity of the modelled soil moisture to corrections that are applied within the processing of the gravity observations. This is shown in this study using different global hydrological corrections. The differences between these corrections are reflected in the modelled soil moisture so that the total hydrological effect (local plus global) is almost identical. The total hydrological effects reduce the observed gravity variation by 30%. Moreover, both seasonal as well as short-term variations clearly related to observed hydro-meteorological parameters are minimized. On the other hand, the sensitivity of the modelled soil moisture to gravity corrections implies that the long-term gravity residuals are not suitable for local hydrological studies unless the significant differences between the global hydrological corrections are resolved.

Keywords: superconducting gravimeter, hydrological modelling, soil moisture, global hydrological effects

1. INTRODUCTION

Terrestrial gravity measurements are utilized in geodesy and geophysics for the study of geometrical and physical properties of the Earth. The high time-domain accuracy of 1 nm s^{-2} (*Hinderer et al., 2007*) and the high frequency resolution of the superconducting gravimeter (SG) complies with current requirements in geophysics and geodesy. Time series of gravity variation observed by SG serve for the analysis of a wide range of geophysical phenomena like post-glacial rebound and tectonic movements (*Steffen and Wu, 2011*; *Van Camp et al., 2011*), seismic normal modes (*Banka and Crossley, 1999*; *Van Camp, 1999*), Slichter mode (*Courtier et al., 2000*) or core nutation (*Ducarme el al., 2007*). These analyses require the elimination of all gravity variations unrelated to the studied phenomena. Nowadays, the observed gravity variation is commonly corrected for tides, effects of atmospheric mass movement and the polar motion effect. As shown in numerous studies at different observatories (*Creutzfeldt et al., 2010a*; *Hasan et al., 2006*; *Hinderer et al., 2012*; *Longuevergne et al., 2009*; *Virtanen et al., 2006*), the gravity variation after these corrections is strongly influenced by hydrological variation. However, these studies rely on directly observed hydrological parameters, particularly on the in situ soil moisture observations. This also applies to the studies that used the gravity observations for hydrological purposes, i.e. for an evaluation or a calibration of local hydrological models (*Creutzfeldt et al., 2010b; Creutzfeldt et al., 2012; Naujoks et al., 2010*). Therefore, methods presented in those studies are not applicable at data-poor sites like in Vienna. To overcome this problem, a novel approach that utilizes global hydrological model outputs and gravity residuals in the calibration process of a local soil moisture model was designed. The gravity residuals are used to eliminate time periods where the soil moisture provided by the global hydrological model does not lead to a reduction of gravity variations. Consequently, this approach requires a partial correlation between the gravity residuals and soil moisture variations interpolated from the global model. Nevertheless, the modelled soil moisture primarily relies on observed air temperature, precipitation and snowmelt. To demonstrate the dependency of the calibration output on gravity residuals, we tested two global hydrological corrections computed using different global hydrological models. Six global models in total were used to estimate the uncertainty related to the corresponding corrections.

Figure 1 depicts the local digital elevation model including the location of the SG (black dot). The SG GWR C025 was in operation from August 1995 to October 2007. During these twelve years, the SG was located in an underground laboratory of the Central Institute for Meteorology and Geodynamics in an outer district of Vienna. The sensor was approximately 8 m below the terrain surface. Eight boreholes in the close vicinity of the building show fine sand and silty sediments. The results from the nearest borehole are shown in Fig. 2. For further computations, we used the transition from sandy silt to clayey silt soil texture found in these boreholes at the depth of 4.1 m as the maximum depth of the soil moisture variation. The input data are described in the following section. The third section of this paper deals with the estimation of global hydrological effects. The approach used for the computation of the local hydrological effect is described in the fourth section. The last two sections present achieved results and conclusions.

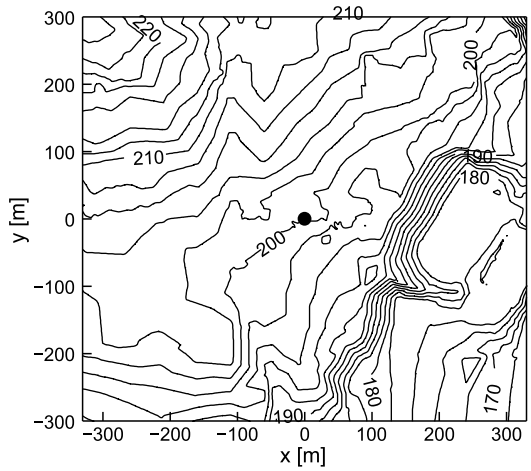

Fig. 1. Local digital elevation model and the location of the superconducting gravimeter (black dot).

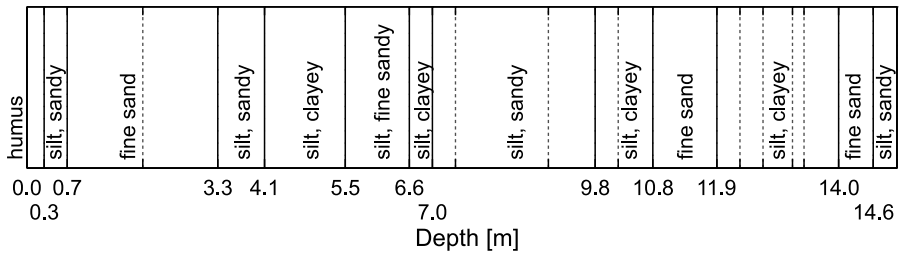

Fig. 2. Soil textures acquired from the borehole nearest to the superconducting gravimeter (10 m away). The vertical full lines represent different soil textures and the dashed lines different soil colours.

2. DATA ACQUISITION

2.1. Gravity variation

Within the data processing, the observed gravity variation was decimated from one second to one hour samples and corrected for Earth tides, atmospheric effect, polar motion, length of day and tidal as well as non-tidal ocean loading effects. The gravity variations corrected in such manner are denoted as gravity residuals hereafter. Most of the corrections can be achieved on an accuracy level better than that of the SG data in the time-domain, others are less accurate. Nevertheless it is good practice to consider all effects as long as data is available and the correction can be done with reasonable effort. The introduced tidal correction was based on tidal parameters estimated from the tidal analysis of observed gravity variations. The computation of the atmospheric correction was based on the ERA Interim surface and pressure level model provided by the European

Centre for Medium-Range Weather Forecasts (*Dee et al., 2011*). The atmospheric correction was computed up to 47 km altitude for the whole globe. The attraction part of the 3D atmospheric density model was computed by a tesseroid approximation described in *Heck and Seitz (2007)* while the loading part was based on Green's functions for the atmospheric loading described in *Merriam (1992)*. Due to the deficient spatial (0.75°) and temporal resolution (12-hour) of the global atmospheric model, a difference between the in situ and ERA Interim pressure was used as an additional correction with a single admittance factor equal to -3 nm s^{-2}/hPa. We used the 12-hour ERA Interim data as the difference between atmospheric effects computed using 6-hour and 12-hour are small. Compared to the ATMACS atmospheric correction (*Klügel and Wziontek, 2009*), the inclusion of the ERA Interim model enables to analyse longer time series without a significant loss of precision. The comparison of our atmospheric correction to the ATMACS correction yielded a standard deviation of only 2.5 nm s^{-2} (for the time period 2004–2007). The polar motion effect and the length of day effect were computed using the EOP Combined Series provided by the International Earth Rotation and Reference System Service. The non-tidal ocean loading effect was based on monthly ECCO-JPL (Estimation of the Circulation and Climate of the Ocean, Jet Propulsion Laboratory solution) model solutions (*Fukumori, 2002*; *Kim et al., 2007*). The use of monthly solutions is possible due to the small difference compared to the diurnal values for the studied region (standard deviation around 0.7 nm s^{-2}). Finally, a linear trend of the SG was subtracted. The high site noise level at Vienna prevented deriving the SG drift model based on absolute gravity measurements. Therefore the trend was estimated by a least square adjustment using time series between 2000 and 2007. Such an approach may remove essential geophysical signals related to the gravity trend, but the main focus of this paper is the study of hydrological effects.

2.2. Hydro-meteorological parameters

No soil moisture or groundwater measurements are available in the close vicinity of the SG. However, groundwater table observations from a 1 km distant station could be utilized. The altitude difference between the underground SG and the groundwater level logger site is 9 m. Provided the distant station reflects somehow the groundwater level at the SG site, the altitude difference to the groundwater level does not play a significant role when calculating the gravitational effect. The effect is close to the Bouguer plate effect, i.e. it does not depend on the vertical distance to the plate but on the thickness of the plate. A problem might arise from an amplitude difference and a phase shift between the groundwater variations observed at different sites. The groundwater variations at four closest sites to the SG in Vienna are shown in Fig. 3. The right panel of this figure shows the distance and the altitude difference between the groundwater loggers and the SG sensor. The observed amplitude of the water table variation is relatively small. The comparison of two nearest groundwater loggers (GW 1 and GW 2) shows minimum phase shift and a maximal amplitude difference of 0.3 m. In terms of the gravitational effect, a specific yield of 3% (see section 4.1 for the specific yield determination) would lead to a difference of 3.8 nm s^{-2}. Therefore, only groundwater measurements of the GW 1 logger with the best time coverage were used.

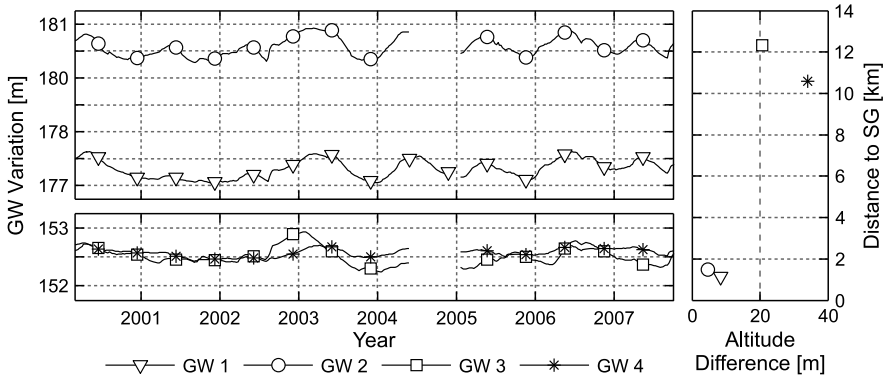

Fig. 3. Observed groundwater (GW) variation at four sites closest to the superconducting gravimeter (SG) in Vienna (left). The right plot shows the distance and the altitude difference of the boreholes from the SG.

The snow height as well as the meteorological observations, i.e. air temperature and precipitation, were recorded by sensors located close to the SG. The snow water equivalent was estimated from the observed snow height via an empirical approach described by *Lundberg et al. (2006)*. Two other approaches were tested (*Jonas et al., 2009*; *Marchand, 2003*), but these methods led to unrealistic results compared to the gravity residuals. In this study, we neglected the effect of the Danube water level variations due to missing observations. This is justified as the corresponding gravity effect has been estimated at 0.65 nm^{-2} per one meter of a water level increase. The maximal gravitational effect of the Danube water level variation was estimated at less than 3 nm s^{-2} for the extreme event in 2002 (*Meurers, 2006*). The soil moisture model is described in Section 4.2.

3. GLOBAL HYDROLOGICAL EFFECTS

From the physical point of view, the hydrological effect on gravity can by divided into a direct (gravitational) and an indirect (loading) effect. Additionally, the hydrological effects on gravity can be separated with respect to the distance between the SG and the hydrological mass into a local and a global part. This separation has no physical meaning but is advisable due to the different calculation procedures. The local effect usually requires detailed models while the calculation of global effect allows lower degree of the approximation. The threshold choice between the local and global part depends on the spatial resolution and quality of the input datasets. Another factor is the effect of topography and the Earth's curvature. It is convenient to set the threshold to a distance with zero gravity effect, i.e. to a distance where a point with an arbitrary mass causes minimal gravitational and loading effect due to the special geometrical relations. This means that a noticeable difference in the input data (soil moisture or snow) at the border between the local and global area has a minimal effect on the final continental water storage effect. The threshold was set to a spherical distance of 0.1°. The variable gravity

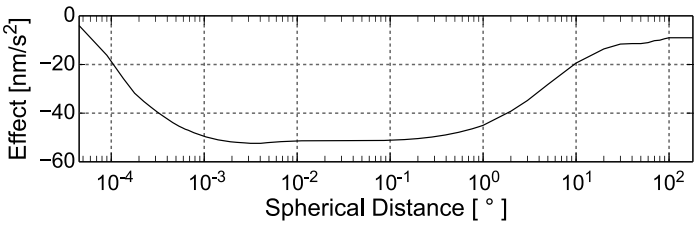

Fig. 4. Gravity effect (attraction + loading effect) of the soil moisture and snow (GLDAS/NOAH model, *Rodell et al., 2004*) at the Vienna superconducting gravimeter station as a function of integration radius (spherical distance).

effect is shown in Fig. 4 where the integration radius is expressed as spherical distance. The computation was based on the soil moisture and snow provided by the GLDAS/NOAH model (*Rodell et al., 2004*) considering the difference between 15/02/2003 and 15/08/2003 (maximal observed water storage change). The transition from the descending to the ascending part of the relation between gravity effect and the integration radius is typical for underground SG installations. The local and global effects interfere and the gravity residuals (without hydrological corrections) are relatively small compared to observations performed with SGs installed above the ground (*Longuevergne et al., 2009*).

The global hydrological effect was analysed using five different hydrological models with daily (or higher) temporal resolution. Namely four land surface models of the GLDAS (CLM, MOS, NOAH, VIC) and the ERA Interim (surface level) model. These models provide information on the soil moisture variation and snow (snow water equivalent). The water stored in the vegetation was neglected as its contribution to the gravity variations is below 0.1 nm s^{-2}. None of these models explicitly includes the groundwater storage. Therefore, the WaterGAP Global Hydrology Model (WGHM) was utilized for the comparison. This model provides information on the total continental water storage, i.e. the sum of the soil moisture, snow, groundwater as well as the surface water (*Döll et al., 2003*). Contrary to the GLDAS and ERA Interim models, only monthly solutions were available for WGHM.

The gravity response to a given water amount was based on the Green's function formalism described in *Farrell (1972)*, where the loading part was computed using load Love numbers given by *Pagiatakis (1988)*. A digital elevation model was included for points with a spherical distance up to 1°. The ERA Interim model covers also the area of Antarctica. However, values for this area as well as for Greenland were not included in the computation due to the missing ice sheet model and forcing data in the GLDAS model (*Rodell et al., 2004*). Omitting parts of a hydrological model together with a model initialisation period result in a trend of the total amount of water stored in the system. This effect was minimized in accordance with the GGP Loading Service (*Boy et al., 2006*; *http://loading.u-strasbg.fr/GGP/*). The water excess or deficit, computed as a sum of all grid cells and compared to long term average (2000–2010), was distributed as a uniform layer over all oceans and seas. This procedure affects the seasonal and the inter-annual variation related to the ocean-continent water exchange. Using the GLDAS/NOAH model,

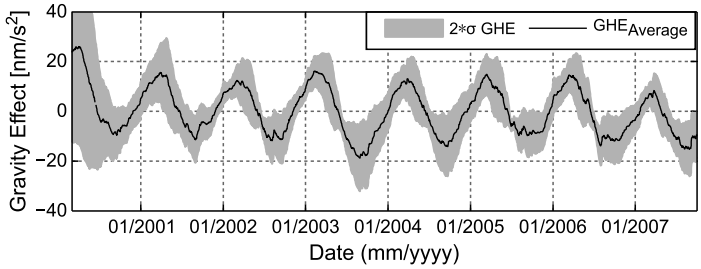

Fig. 5. Average global gravity effect at the Vienna superconducting gravimeter station derived from six different hydrological models. The grey colour represents the confidence bounds of 95% ($2\sigma GHE$, *GHE* is the global global hydrological effect).

the seasonal amplitude of the corresponding gravity effect was estimated at 3.1 nm s^{-2} and the trend (inter-annual) at 0.7 nm s^{-2}/year.

Figure 5 shows the average global hydrological effect (GHE_{Average}) computed using all GLDAS models and the ERA Interim model. The depicted time series starts in February 2000 as this is the starting epoch of the GLDAS/NOAH (0.25°) model. The confidence bounds (95%) show the significant discrepancy between these models. The increased dispersion before 2002 is caused by anomalous behaviour of the GLDAS/MOS model. More specifically, it is related to the insufficiently accurate elimination of the trend in the water amount stored in the system. The differences get smaller after 2002 but they are still considerable. The difference between the GLDAS/MOS and the GLDAS/CLM model reaches 17 nm s^{-2} in October 2003. Table 1 presents the standard deviation of differences of each model to the average variations over the whole time span as well as over the time span starting after 2002. For comparison purposes, we also included the WGHM model. This model was omitted from the average computation because of its low temporal resolution (one month). Nevertheless, the gravity effect computed from this model is similar to GLDAS and ERA models despite the inclusion of different water storage compartments. For the GLDAS/NOAH model, the standard deviation of the difference between maximal available time resolution, i.e. 3-hour, and

Table 1. Standard deviation (in nm s^{-2}) of different global hydrological effects compared to the average variation between 2000–2008 and 2002–2008. The average variation was computed from all models except WGHM which was available only in monthly time resolution (data in italics).

Model	2000–2008	2002–2008
GLDAS/CLM	4.5	4.2
GLDAS/MOS	8.0	3.9
GLDAS/NOAH	2.9	1.8
GLDAS/VIC	3.3	3.2
ERA Interim	3.9	3.1
WGHM	*3.5*	*2.5*

one month is around 0.8 nm s^{-2}. The maximum difference between the GLDAS/NOAH model with 0.25° and 1° resolution is 1.5 nm s^{-2} (standard deviation 0.6 nm s^{-2}).

4. LOCAL MODEL

4.1. Gravity response

The gravity response to snow, soil moisture and groundwater variations was computed using a prism approximation. A digital elevation model including artificial objects was used for this purpose. This allows to take into account the effect of snow on the roof and exclude the soil moisture effect of layers beneath the nearest buildings and within the first meter below roads and car parks. The groundwater effect was computed using data observed at the GW 1 site (see Fig. 3). This groundwater level variation was used for the whole area considering the elevation model and maximal depth of the soil moisture layers. This approach ensures that the groundwater level does not exceed the actual terrain and that the contribution of unsaturated zone is consistent with the saturated zone. A specific yield of 3% was used for the computation of the groundwater effect. This is a minimum value for a silt given by *Johnson (1967)*. The reason for choosing this low value is the anti-correlation of observed groundwater variation and gravity residuals, which would indicate a negative value of the specific yield. One possible explanation of the anti-correlation is the dominance of the soil moisture effect with similar temporal variation as in the observed groundwater.

To assess the contribution of the snow height dependency on altitude, we computed the gravity response to snow considering a gradient of 5 cm snow height increase per 100 m in altitude. As shown by *Mörikofer (1948)*, the gradient strongly depends on time and the catchment. Nevertheless, neglecting the altitude dependence of the snow height changes the maximum gravitational effect by only 0.5 nm s^{-2}. To account for possible spatial patterns of the soil moisture related the topography, we computed the gravity response to the soil moisture extrapolated in the local zone by means of a topographic wetness index (*Moore et al., 1991*). The maximal possible factor of the soil moisture change within the radius of 300 m from the SG due to the topography was set to 1.2 (with respect to SG location). A maximal amplitude change of 1.6 nm s^{-2} (1.5%) was found by the comparison with the effect of constant soil moisture layers in the horizontal direction. This is due to the relatively flat topography within the first 100 m surrounding the SG (see Fig. 1). Therefore, the further computations do not take into account the topography-based spatial variability of the soil moisture and snow.

4.2. Hydrological modelling

The missing soil moisture observations were substituted by modelled values using in situ precipitation, air temperature and snow water equivalent. The soil moisture variation was simulated by the soil water balance subroutine of the rainfall-runoff model MISDc described in *Brocca et al. (2008)*. The unknown model parameters, namely the water capacity, wetting front soil suction head, hydraulic conductivity, initial soil moisture condition, pore size distribution index and evaporation parameter need to be obtained by means of the model calibration. In an ideal situation, the conceptual hydrological model

would be calibrated against the observed soil moisture. As a consequence of the missing in situ observations, a novel procedure was designed in this study. It combines the soil moisture variations provided by a global hydrological model and the gravity residuals. The idea is to use only those time intervals where the soil moisture gravity effect based on the global model leads to a decrease of gravity variations. We used the global hydrological model with highest spatial resolution, i.e. the GLDAS/NOAH (0.25°) model. The linearly interpolated soil moisture is hereafter denoted as a priori soil moisture. This procedure assumes the global model to be representative for the given region and the residuals to be corrected for all major sources of gravity variations not related to the soil moisture. The first assumption limits the analysis to relatively flat and homogeneous areas. Otherwise, no or only very short time intervals of a priori soil moisture variation would match the gravity residuals. The second assumption requires the correction of gravity residuals for a local groundwater, snow as well as global hydrological effects as described in Sections 4.1 and 3 respectively.

In the first step, the gravity response to a priori soil moisture variation was computed. The gravity residuals were then corrected for this effect and other hydrological effects, i.e. average global hydrological effect, snow and groundwater. In the next step, the time intervals where these hydrological effects led to gravity residuals smaller than 5 nm s^{-2} were identified. Due to this procedure, two thirds of the eight and a half year long soil moisture time series were eliminated. Only the remaining a priori soil moisture variation was then used for the calibration. All calibration parameters listed above were estimated via minimizing the differences between the a priori and the modelled soil moisture. A non-linear optimization was utilized for this purpose. The initial soil moisture condition was constrained to fit the gravity residuals at the beginning of the time series, i.e. the gravity effect of the estimated initial soil moisture reduced the gravity residuals to ± 5 nm s^{-2} (corresponds to 40–44% soil moisture). Table 2 shows the upper and lower limits for the remaining parameters as well as the estimated values. These limits were set in accordance to *Brocca et al., (2008)* and *Todd and Mays (2005)*. The calibration of the model was performed for one layer in an average depth of 0.2 m. Subsequently, an exponential function with an exponent equal to $-1.058\ m^{-1}$ was used to describe the attenuation of the soil moisture variation up to the transition from sandy silt to clayey silt

Table 2. Hydrological parameters of the local conceptual model. The *Min* and *Max* values represent the upper and the lower limits used for the calibration. The column *Average* refers to the a priori soil moisture selected using the average global hydrological correction. Similarly, CLM refers to the GLDAS/CLM correction. * refers to the settings used for the GLDAS/CLM model.

Parameter	*Min*	*Max*	*Average*	CLM*
Initial soil moisture [%]	40 (35*)	44 (39*)	40	35
Field capacity [%]	10	45	28	39
Hydraulic conductivity [mm/h]	1	25	12.8	12.9
Soil suction head [mm]	25	375	200	200
Pore size distribution index	0.05	1	0.15	0.17
Evaporation parameter	1.4	2.4	2.4	2.4

soil. This decay rate was estimated using average (2000–2007) a priori soil moisture variations for each GLDAS layer and the maximum depth of the unsaturated zone (4.1 m). No interaction between the saturated and unsaturated zone was modelled. Finally, the gravity response to the modelled (after calibration) soil moisture was computed.

To assess the impact of the corrections applied prior to the calibration, the whole procedure was also performed for the global hydrological effect based on the GLDAS/CLM model. The use of this hydrological model results in the smallest seasonal amplitude of the global effect compared to the average variations. The amplitude is about 43% smaller. This means that the resulting gravity variation after the subtraction of the global hydrological effect will also have smaller amplitude. This is related to the underground installation of the SG in Vienna (see Fig. 4). The following section discusses the consequences of the use of different global hydrological effects.

5. RESULTS AND DISCUSSION

Figure 6 shows the local hydrological effect superimposed on the gravity residuals. The upper part of the figure shows the gravity residuals corrected for the average global hydrological effect (GHE_{Average}). The lower part of the figure shows the gravity residuals corrected for GLDAS/CLM global hydrological effect ($GHE_{\mathrm{GLDAS/CLM}}$). The seasonal amplitude of the local hydrological effect is different in both parts. This is due to the coupling of the model calibration to gravity residuals. The use of different corrections applied prior to the calibration results in the selection of different time intervals of the a priori soil moisture. The calibration algorithm aims to minimize the differences between the a priori and modelled soil moisture. Nevertheless, the modelled soil moisture always reflects observed precipitations, snow and temperature variations. The subtraction of different hydrological effects influences primarily the amplitude and to a lesser extend the phase of the calibrated soil moisture variation. A different specific yield would affect the

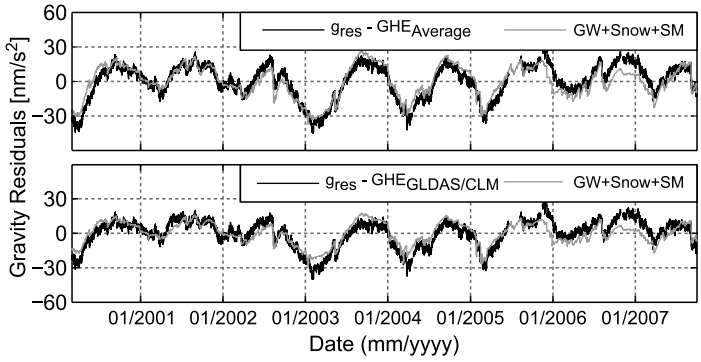

Fig. 6. Gravity residuals and the local hydrological effect. The local gravity effect consist of modelled soil moisture (SM), groundwater (GW) and snow. The upper plot is related to the average global hydrological effect ($g_{res} - GHE_{\mathrm{Average}}$) and the lower plot to the GLDAS/CLM global hydrological effect ($g_{res} - GHE_{\mathrm{GLDAS/CLM}}$).

results in a similar way. The significant differences between the global hydrological corrections (see Table 1) imply that the obtained results are not suitable for hydrological purposes.

Figure 7 shows the final gravity residuals after the subtraction of all computed effects, i.e. the average global hydrological effect, modelled soil moisture, groundwater and snow. The utilization of the GLDAS/CLM model would result in almost identical corrected gravity variation. The different global hydrological effect is compensated by the modelled soil moisture effect (see Fig. 6). The subtraction of computed hydrological effects reduces the standard deviation of gravity residuals by more than 30% from 9.5 to 6.6 nm s^{-2}. The introduced hydrological corrections reduce the amplitude of the seasonal and inter-annual variations. More importantly, the short-term variations, visible in the uncorrected gravity residuals and clearly related to the rain or snow effects, are reduced. This is shown in Fig. 8 where three selected rain events are depicted. The residual gravity feature visible in Fig. 7 at the end of 2005 was not significantly affected by the subtraction of hydrological effects. The observed precipitation, snow or groundwater do not show any anomalous events for this time period. The introduced global hydrological effect and the non-tidal ocean loading effect do not cover the whole Earth and all hydrological components. No gravity effect for Greenland, Antarctica, Arctic Ocean or glaciers was considered. However, it can be assumed that the inclusion of these areas would only affect long term gravity variations. As mentioned in Section 2.2, the neglected contribution of the Danube water level variation should not exceed 3 nm s^{-2}. It is therefore doubtful that this variation is related to hydrological effects. It is more likely due to SG issues (two observation interruptions from July 2005 to December 2005). Additional improvement of gravity residuals can be expected after using an atmospheric correction based on higher resolution weather models.

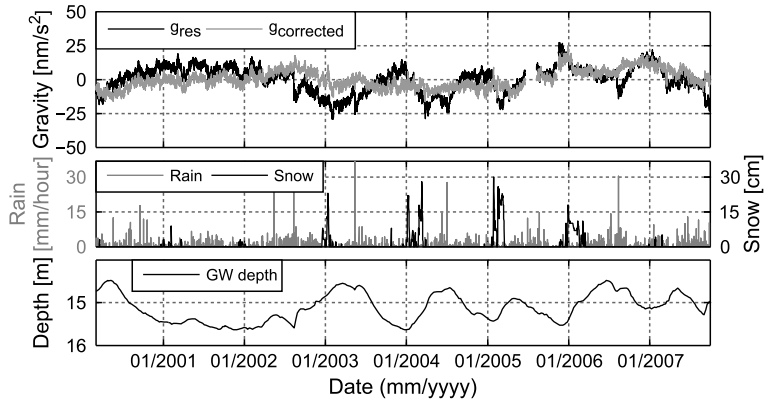

Fig. 7. Gravity residuals before (g_{res}) and after the subtraction of calculated hydrological effects ($g_{corrected}$). The middle plot shows the observed rain rate and snow depth while the bottom plot shows the depth of the groundwater (GW) table referenced to the altitude of the superconducting gravimeter sensor.

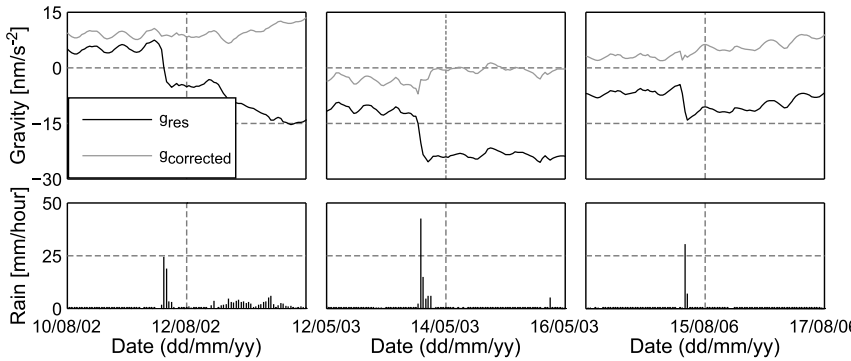

Fig. 8. Short term gravity variations before (g_{res}) and after the subtraction of calculated hydrological effects ($g_{corrected}$). The lower plot shows the observed rain rate.

6. CONCLUSIONS

We have computed the hydrological effects on gravity for the superconducting gravimeter at the Vienna station. Due to the lack of in situ soil moisture measurements, we developed a novel approach for computing the local soil moisture effect. This approach combines gravity residuals, a priori soil moisture variations acquired from a global hydrological model, in situ temperature, precipitation and snow height time series. The gravity residuals are used to select those time periods where the a priori soil moisture leads to a reduction of the gravity residuals. Only these time periods are then used for the calibration of the local conceptual model. The proposed approach is applicable for all gravimeter sites without in situ soil moisture measurements provided these are located in relatively flat and homogenous regions. Otherwise, the algorithm would fail to identify time intervals where the a priori soil moisture leads to the reduction of gravity residuals. To test the sensitivity of this approach to gravity corrections applied prior to the calibration process, we used two different global hydrological corrections. The results showed that the total hydrological correction is almost identical despite the use of different global hydrological corrections. This is related to the nature of the calibration algorithm which tends to minimize the differences between input and output soil moisture variations provided these variations can be reproduced by the water balance routine using observed precipitation, snowmelt and temperature. This also means that the modelled soil moisture will always strongly depend on applied corrections and therefore is not suitable for hydrological purposes. The computed total hydrological correction reduces the variation of gravity residuals by 30% and minimizes both seasonal and short term variations related to hydrological processes.

Acknowledgements: The authors thank the Geophysical and Climatological Divisions of the Central Institute for Meteorology and Geodynamic (Austria), Andreas Güntner (GFZ German Research Centre for Geosciences), Prof. Döll's working group (Institute of Physical Geography, Goethe University) as well as Peter Janac (Vienna City Administration, Municipal Department 45 - Water Engineering) for data provision. The data used in this study were acquired as part of the mission of NASA's Earth Science Division and archived and distributed by the Goddard Earth

Sciences (GES) Data and Information Services Center (DISC). The ECCO Ocean Bottom Pressure data were acquired from *http://grace.jpl.nasa.gov*. The authors thank the Agency of the Ministry of Education, Science, Research and Sport of the Slovak Republic for the Structural Funds of EU and Slovak University of Technology in Bratislava for financial support of the Project ITMS 26220220108. Remarks and suggestions by two anonymous reviewers helped to improve this paper.

References

Banka D. and Crossley D., 1999. Noise levels of superconducting gravimeters at seismic frequencies. *Geophys. J. Int.*, **139**, 87–97.

Boy J.-P. and Hinderer J., 2006. Study of the seasonal gravity signal in superconducting gravimeter data. *J. Geodyn.*, **41**, 227–233.

Brocca L., Melone F. and Moramarco T., 2008. On the estimation of antecedent wetness conditions in rainfall–runoff modelling. *Hydrol. Process.*, **22**, 629–642.

Courtier N., Ducarme B., Goodkind J., Hinderer J., Imanishi Y., Seama N., Sun H., Merriam J., Bengert B. and Smylie D.E., 2000. Global superconducting gravimeter observations and the search for the translational modes of the inner core. *Phys. Earth Planet Inter.*, **117**, 3–20.

Creutzfeldt B., Güntner A., Wziontek H. and Merz B., 2010a. Reducing local hydrology from high-precision gravity measurements: a lysimeter-based approach. *Geophys. J. Int.*, **183**, 178–187.

Creutzfeldt B., Güntner A., Vorogushyn S. and Merz B., 2010b. The benefits of gravimeter observations for modelling water storage changes at the field scale. *Hydrol. Earth Syst. Sci.*, **14**, 1715–1730.

Creutzfeldt B., Ferré T., Troch P., Merz B., Wziontek H. and Güntner A., 2012. Total water storage dynamics in response to climate variability and extremes: Inference from long-term terrestrial gravity measurement. *J. Geophys. Res.-Atmos.,* **117**, D08112.

Dee D.P., Uppala S.M., Simmons A.J., Berrisford P., Poli P., Kobayashi S., Andrae U., Balmaseda M. A., Balsamo G., Bauer P., Bechtold P., Beljaars A.C.M., van de Berg L., Bidlot J., Bormann N., Delsol C., Dragani R., Fuentes M., Geer A.J., Haimberger L., Healy S.B., Hersbach H., Hólm E.V., Isaksen L., Kållberg P., Köhler M., Matricardi M., McNally A.P., Monge-Sanz B.M., Morcrette J.J., Park B.K., Peubey C., de Rosnay P., Tavolat C., Thépaut J.N. and Vitart F., 2011. The ERA-Interim reanalysis: configuration and performance of the data assimilation system. *Q. J. Roy. Meteor. Soc.*, **137**, 553–597.

Döll P., Kaspar F. and Lehner B., 2003. A global hydrological model for deriving water availability indicators: model tuning and validation. *J. Hydrol.*, **270**, 105–134.

Ducarme B., Sun H.-P. and Xu J.-Q., 2007. Determination of the free core nutation period from tidal gravity observations of the GGP superconducting gravimeter network. *J. Geodesy*, **81**, 179–187.

Farrell W.E., 1972. Deformation of the Earth by surface loads. *Rev. Geophys.*, **10**, 761–797.

Fukumori I., 2002. A Partitioned Kalman Filter and Smoother. *Mon. Weather Rev.*, **130**, 1370–1383.

Hasan S., Troch P.A., Boll J. and Kroner C., 2006. Modeling the hydrological effect on local gravity at Moxa, Germany. *J. Hydrometeorol.*, **7**, 346–354.

Heck B. and Seitz K., 2007. A comparison of the tesseroid, prism and point-mass approaches for mass reductions in gravity field modelling. *J. Geodesy*, **81**, 121–136.

Hinderer J., Crossley D. and Warburton R.J., 2007. Gravimetric methods - superconducting gravity meters. In: Schubert G. (Ed.), *Treatise on Geophysics,* **3**. Elsevier, Amsterdam, 65–122.

Hinderer J., Pfeffer J., Boucher M., Nahmani S., Linage C., Boy J.P., Genthon P., Seguis L., Favreau G., Bock O. and Descloitres M., 2012. Land water storage changes from ground and space geodesy: first results from the GHYRAF (Gravity and Hydrology in Africa) experiment. *Pure Appl. Geophys.*, **169**, 1391–1410.

Johnson A.I., 1967. *Specific Yield-Compilation of Specific Yields for Various Materials*. Water Supply Paper 1662-D. United States Government Printing Office, Washington, D.C.

Jonas T., Marty C. and Magnusson J., 2009. Estimating the snow water equivalent from snow depth measurements in the Swiss Alps. *J. Hydrol.*, **378**, 161–167.

Kim S.-B., Lee T. and Fukumori I., 2007. Mechanisms controlling the interannual variation of mixed layer temperature averaged over the Niño-3 region. *J. Climate*, **20**, 3822–3843.

Klügel T. and Wziontek H., 2009. Correcting gravimeters and tiltmeters for atmospheric mass attraction using operational weather models. *J. Geodyn.*, **48**, 204–210.

Longuevergne L., Boy J. P., Florsch N., Viville D., Ferhat G., Ulrich P., Luck B. and Hinderer J., 2009. Local and global hydrological contributions to gravity variations observed in Strasbourg. *J. Geodyn.*, **48**, 189–194.

Lundberg A., Richardson-Näslund C. and Andersson C., 2006. Snow density variations: consequences for ground-penetrating radar. *Hydrol. Process.*, **20**, 1483–1495.

Marchand W., 2003. *Applications and Improvement of a Georadarsystem to Assess Areal Snow Distribution for Advances in Hydrological Modelling*. Ph.D. Thesis, Norwegian University of Science and Technology, Trondheim, Norway.

Merriam J.B., 1992. Atmospheric pressure and gravity. *Geophys. J. Int.*, **109**, 488–500.

Meurers B., 2006. Long and short term hydrological effects on gravity in Vienna. *Bulletin d'Information des Marées Terrestres*, **142**, 11343–11351.

Moore I.D., Grayson R.B. and Ladson A.R., 1991. Digital terrain modelling: A review of hydrological, geomorphological, and biological applications. *Hydrol. Process.*, **5**, 3–30.

Mörikofer W., 1948. The dependence on altitude of the snow cover in the Alps. In: *Proceedings Union Géodésique et Géophysique*, Oslo, 161–170.

Naujoks M., Kroner C.,Weise A., Jahr T., Krause P. and Eisner S., 2010. Evaluating local hydrological modelling by temporal gravity observations and a gravimetric three-dimensional model. *Geophys. J. Int.,* **182**, 233–249.

Pagiatakis S. D., 1988. *Ocean Tide Loading on a Self-Gravitating, Compressible, Layered, Anisotropic, Viscoelastic and Rotating Earth with Solid Inner Core and Fluid Outer Core*. Technical Report 139. University of New Brunswick, Fredericton, Canada.

Rodell M., Houser P. R., Jambor U., Gottschalck J., Mitchell K., Meng C. J., Arsenault K., Cosgrove B., Radakovich J., Bosilovich M., Entin J.K., Walker J.P., Lohmann D. and Toll D., 2004. The Global Land Data Assimilation System. *Bull. Am. Meteorol. Soc.*, **85**, 381–394.

Steffen H. and Wu P., 2011. Glacial isostatic adjustment in Fennoscandia - A review of data and modeling. *J. Geodyn.*, **52**, 169–204.

Todd D.K. and Mays L.W., 2005. *Groundwater Hydrology.* 3rd Edition. John Wiley and Sons, Inc. Hoboken, NJ.

Van Camp M., 1999. Measuring seismic normal modes with the GWR C021 superconducting gravimeter. *Phys. Earth Planet Inter.*, **116**, 81–92.

Van Camp M., de Viron O., Scherneck H.-G., Hinzen K.-G., Williams S.D.P., Lecocq T., Quinif Y. and Camelbeeck T., 2011. Repeated absolute gravity measurements for monitoring slow intraplate vertical deformation in western Europe. *J. Geophys. Res.-Sol. Earth*, **116**, B08402.

Virtanen H., Tervo M. and Bilker-Koivula M., 2006. Comparison of superconducting gravimeter observations with hydrological models of various spatial extents. *Bulletin d'Information des Marées Terrestres*, **142**, 11361–11368.